ABCM Symposium Series in Mechatronics - Vol. 3 - pp.586-594

DEEP UV LITHOGRAPHY VALVELESS MICROPUMP DESIGN AND TEST

Eurípedes G. O. Nóbrega, egon@fem.unicamp.br
R. Mendeleyev, sn
13087-970 Campinas SP
Faculty of Mechanical Engineering
State University of Campinas

Camila Dalben Madeira Campos, camilac@fea.unicamp.br
R. Monteiro Lobato, 80
13087-970 Campinas SP
Faculty of Food Engineering
State University of Campinas

Abstract. *Microelectromechanical systems have been receiving worldwide attention from researchers in the last two decades, due to the high potential of new products development. Between these new products, micropumps are one of the more important new devices used to precisely control very small fluid flows. They have been used, for example, in chromatography, to apply insulin doses, in DNA recognition microdevices, and to control specific chemical reactions. Valveless micropumps are benefited from the reduced dimensions, resulting in smaller manufacturing cost and higher lifetime, due to excluding moving parts. Using deep UV lithography, a recently applied technique to microsystems manufacturing presents several advantages over traditional techniques, and it was used to build low-cost prototypes based on polyuretane-acrilate. The design, construction and testing of a micropump prototype is described in the paper. A testbed was implemented to evaluate the pump performance and its details and experimental results are presented, showing performance similar to designs presented in the literature, with good flow and pressure relations.*

Keywords: *Microelectromechanical systems, micropumps, micromechatronics*

1. INTRODUCTION

Regarding the origins of microelectromechanical systems (MEMS), measurements of piezoresistivity coefficients in germanium and silicon published early as 1954 pointed the way for future pressure, displacement, and strain sensors design (Smith, 1954). But some authors claim that a famous talk and respective publishing by Feynman (1960) revealed the possibilities of nanotechnology and micromechanical systems. From 1960 to 1970, resonant gate transistors (Nathanson *et al*, 1967), accelerometers (Royland and Angell, 1978), pressure sensors and silicon based strain sensors were fabricated, and these prototypes are generally considered as the beginning of MEMS device fabrication (O'Connor, 1992). The term micromachining, and also a survey of the respective current major techniques, with potential to be applied to mechanical systems, were first published by Petersen (1982). During the next decades, intensive laboratory explorations followed, and some industrial success cases became well known, like inkjet printer head, strain-based pressure sensors, mechanical resonators, accelerometers and gyroscope automotive sensors.

MEMS devices may include in the same structure the electronic and mechanical modules, encompassing sensors and actuators, with dimensions from the order of micrometers to millimeters. Today, they constitute one of the more promising and fast-growing new technologies (Poel Filho, 2005). In a broad sense, miniaturization results in several new applications, beyond the reach of regular macro scale equipment. A good example is the development of solid state accelerometer used in the new automobile brake systems and air-bags (Ko *et al*, 1995; Yazdi and Najfi, 2000), an application only made possible by the large scale production associated to microfabrication techniques.

MEMS, beginning as an application of microelectronic techniques to build mechanical systems, were first made in silicon. Nowadays, new materials and methods have been tested, looking for good electrical and mechanical properties and low costs. The common methods for MEMS manufacturing are based on micromachining and different kinds of lithography, including the very successful LIGA (Madou, 1997; Ehrfeld, 2003). Micromachining has been largely used in industrial sensor production since the early 1980´s. It is based on different etching techniques used to shape forms on a crystal substrate (O'Connor, 1992). LIGA involves the use of X-ray radiation to transfer a pattern to a polymeric thick layer and build metallic molds using some deposition technique. Using the metal structure so built, plastic copies may be generated using several techniques (Bacher *et al*, 1995). Despite being very efficient, and a great improvement at the time it was developed, the main disadvantage of LIGA is yet a high cost due to mold manufacturing.

Soft lithography, a more recent method, is based on similar principles used by LIGA. It presents lower production cost, but molds are still necessary. In soft lithography a robust polymeric master mold is prepared and then different materials and techniques may be used to replicate it, like UV-radiation exposure and baking. Depending on the desired device, it may involve high costs (Rogers and Nuzzo, 2005).

A new application developed by Fernandes and Ferreira (2006) uses deep UV lithography and polyuretane-acrilate (PA), presenting very low cost and the capacity to implement high aspect ratio structures. It is a soft lithography variation, eliminating the need of molds and simplifying the procedures. UV-radiation is applied to cure the successive PA layers, which are used to assemble the final device. A mask, printed on a simple slide film, is used instead of molds. After exposure, the resin under the black parts in the mask will not become rigid, and may be simply washed out. Several types of devices can be made using this process, like micromixers, microvalves, and micropumps.

Microfluidic systems are very important to chemical analysis and biomedical engineering (Schwarz and Hauser, 2001) and new analysis technologies, as gas chromatography, in which very small volumes must be precisely controlled (Daniel and Guts, 2006). The integration of microfluidic systems, including a number of electromechanical devices, like pumps, valves, sensors, mixers and divisors, are essential to design the so called Lab-On-a-Chip (LOC) systems. These are small systems, commonly made in a single tablet, used to decrease the scale and to increase the efficiency of some biochemical and chemical analysis (Chow, 2002). Their use reduces the cost with reagents, human-labor, and equipments, and also the correspondent analysis time.

New pump designs are among the more important areas in microfluidic devices development. A pioneer work in this field, Smits (1990) designed a micropump to be used in insulin dosage for diabetic patients. Today, several types of micropumps are fundamental components in microfluidic system controls, being responsible for distributing very precise small flows.

Micropumps may be classified based on the actuation principle or on the pumping principle. The actuation principle may be piezoelectric, pneumatic, thermopneumatic, thermomechanical, electrostatic, or electromagnetic while the pumping principle may be alternated, peristaltic, electrohydrodynamic, electrosmotic or ultrasonic, (Zhang, 2005). Also, the pump principle may be positive displacement or continuous flow.

Diaphragm micropumps were first developed with valves, whose actuation depends on hydrostatic pressure. Considering Figure 1, when the pressure decreases in the upper chamber, not shown in the figure, the membrane dilates increasing the pumping chamber volume, resulting in a lower pressure. This pressure decrease makes the input valve to open and the output valve to be pushed against the walls, keeping it closed. When the membrane returns to its initial form, the pressure in the pumping chamber increases, closing the input valve and opening the output valve, letting the fluid flow out (Zengerle *et al* 1995).

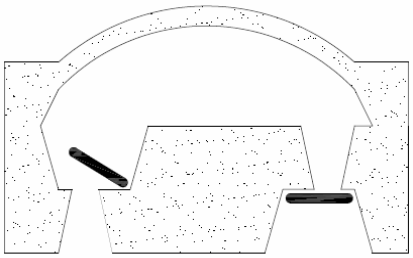

Figure 1: A diaphragm micropump with valves

Stemme and Stemme (1993) developed the first valveless micropump, distinguishable by its simple structure, but producing the same order of outflow than the conventional one. Valveless micropump can be peristaltic, with nozzle/diffuser, ultrasonic, electrosmotic, and electroforetical (Teymoori and Aspour-Sani, 2005; Olsson, 1998; Nguyen *et al*, 2000; Herr *et al*, 1999).

In the diaphragm valveless micropumps the valves are substituted by diffusers/nozzles. Diffusers are channels whose cross section increases in the flow direction decreasing the velocity of the flow and increasing the static pressure of the fluid through the system, turning kinetic energy into potential energy. When the section area decreases, restricting the flow, it is called nozzle. Due to technological reasons, the channel cross section may be a circle or a rectangle, but these forms do not influence the device efficiency (Olsson, 1998). In miniaturized devices, it is common to choose rectangular diffusers, which results in more compact projects (Olsson *et al*, 2000).

The flow inside the device is a consequence of the small effort effect, responding to the membrane deformation. The net flow of the fluid will occur in the direction whose resistance is smaller. Figure 2 presents the two possibilities, with the bigger flow and the opposite flow resulting in the net flow direction. The diffuser can be projected geometrically to cause a pressure decrease smaller then the nozzle (Olsson, 1998).

Considering the scheme represented in Figure 2a, the positive pressure difference applied to the upper chamber causes an expansion of the membrane and a negative variation of the volume of the lower chamber, consequently the expulsion of the same amount of fluid. At this moment, the input channel acts as a nozzle and the output one as a diffuser. The flow is bigger in the diffuser then in the nozzle. When the pressure difference is eliminated (or negative), represented in Figure 2b, the membrane returns to its original form (or expands), causing the fluid to flow in. At this moment, the function of the input and output channels are now the opposite. The result will be a single direction for the net fluid flow (Jiang *et al*, 1998).

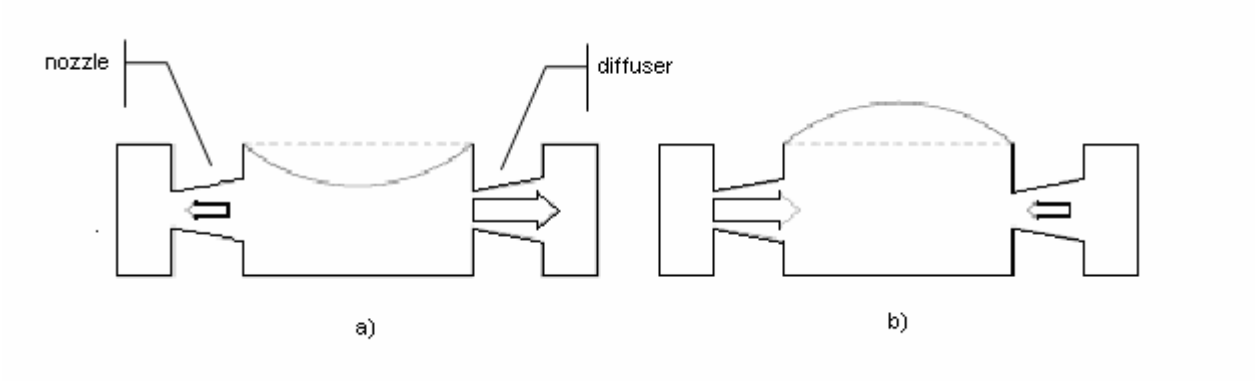

Figure 2: The valveless pump and the resulting net flow direction

In this paper, the design, manufacture and test of a valveless diaphragm micropump is presented, using polyuretane-acrilate as the main structural material and latex for the membrane. The pump design is presented in Section 2 and its manufacture process described in Section 3. An experimental setup built for the test is detailed in Section 4 and the respective results presented and analyzed in Section 5. Final conclusions are in Section 6.

2. MICROPUMP DESIGN

Using PA and deep UV lithography as construction method, the pump here presented is based on the prototype designed by Costa (2006). A schematic drawing is presented in Figure 3.

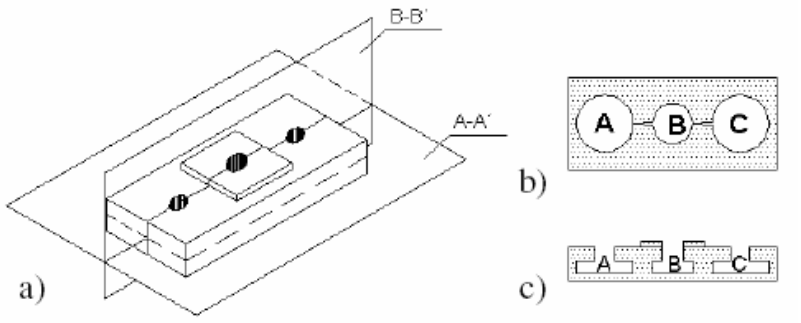

Figure 3: Valveless micropump drawings a) A perspective b) A-A' plane c) B-B' plane

Referring to Figure 3, it may be seen a central chamber, separated by the membrane in two parts: the upper chamber, where the pressure is applied to deform the membrane, and the pumping chamber in the lower part. There are also two other chambers, respectively an input and an output reservoir.

The complete device was designed with 52 mm of length, 23 mm of width and 8.2 mm of height. The pumping lower chamber has 10 mm in diameter and its volume varies according to the deformation of the membrane above it. The reservoirs present a constant volume (14.14 mm diameter and 3.2 mm height). When the membrane is not deformed, the volume of the pumping lower chamber is half of the volume of the reservoirs.

The diffusers were designed with rectangular flat section and rounded edges to decrease the pressure loss, following Yamahata *et al* (2005) and Khoo and Liu (2000) models. Diffusers details can be seen on Figure 4.

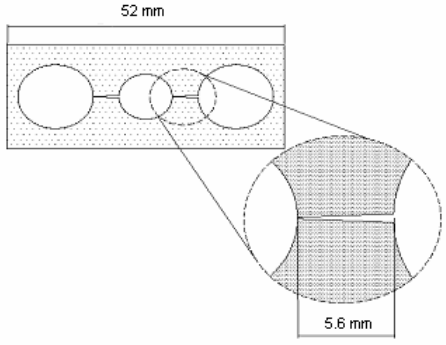

Figure 4: Zoom of the diffuser geometric details

The diffusers base is 520 μm for the bigger side and 100 μm for the smaller one, the channel length is 5.6 mm and its height is 1.6 mm. Stemme and Stemme (1993) calculate the diffuser efficiency using the equation below, and they suggest that, for good efficiency, this relation must be between 1 and 5.

$$n = \frac{E_n}{E_d} = \frac{K_{n,1} + (K_{n,2} + K_{n,3})(A_i / A_o)^2}{K_{d,1} + K_{d,2} + K_{d,3}(A_i / A_o)^2}$$

where E means pressure loss coefficient, K means pressure coefficient and A_i means diffuser input area, A_o means diffuser output area, and the under scripts n and d mean nozzle and diffuser, respectively. For the present design, the relation was found as 4.25.

3. MICROPUMP MANUFACTURE

A complete description of the micropump manufacturing procedure to build each layer and its assembly to form the prototype, including materials and timing, is presented in this section.

Six layers, built with PA, and also the latex membrane, are necessary to fabricate the micropump. In Figure 5, the masks for the UV radiation exposure of each layer are represented. After completely processing the layers, they are assembled successively, including the membrane, to form the pump.

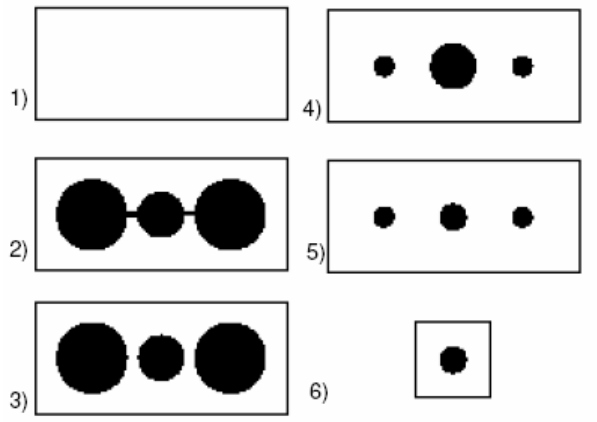

Figure 5: Mask drawings

Two glass plates are used to press the resin, before exposing it to UV-radiation. The first plate, covered with a conventional plastic film to protect from gluing, receives the PA, and the other one receives the printed mask. As the resin is spread over the first glass plate it is necessary to use a mask to induce the cure of the base layer with the wished dimensions. That is the reason for the first white mask. The layer height is determinated by separators between the plates. This setup is then exposed to UV-radiation during seven minutes, forming one of the layers of the device. To unite the layers, two hours exposition is necessary, with a very small amount of PA between then. To include the membrane, made with chirurgical gloves latex, it is used a cianoacrilate glue. The final result can be seen at the photograph presented in Figure 6.

Figure 6: Final prototype

4. EXPERIMENTAL SETUP

At this section, the experimental setup built to test the prototype is presented. The main objective of the testing system is to apply a controlled range of pressures to the upper chamber of the diaphragm, filled with ambient air, and originally at ambient pressure. This setup is depicted in Figure 7.

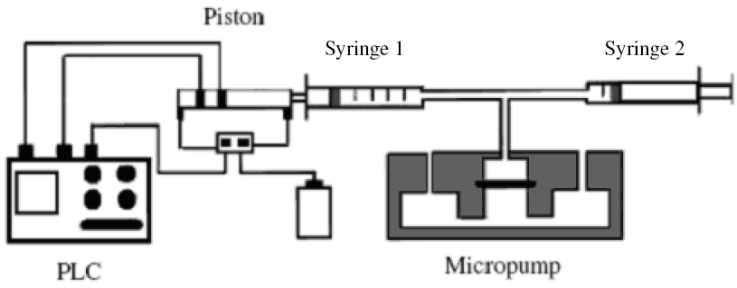

Figure 7: Experimental setup to evaluate the micropump performance

It may be seen in Figure 7 an industrial programmable logic controller (PLC), a double action pneumatic cylinder and respective position sensors and control valve, an arrangement with some flexible tubes and a pair of syringes, and also the tested micropump.

The piston movement in the pneumatic cylinder is controlled by the PLC, in order to maintain always the some displacement, based on the position of the sensors. This movement is transmitted to the first syringe, causing a volume variation of the air in the upper chamber of the membrane. By proper positioning of the second syringe, a specified amount of volume variation is transformed in pressure variation and deformation of the membrane, and consequently the flow of the fluid in the lower membrane chamber. The frequency and the number of piston strokes are also controlled by the PLC. The pumped fluid is collected and then weighted after the last stroke. The two syringes present the same maximum volume of 10 ml.

The ladder diagram of the PLC programming to control the pneumatic cylinder is presented in Figure 8.

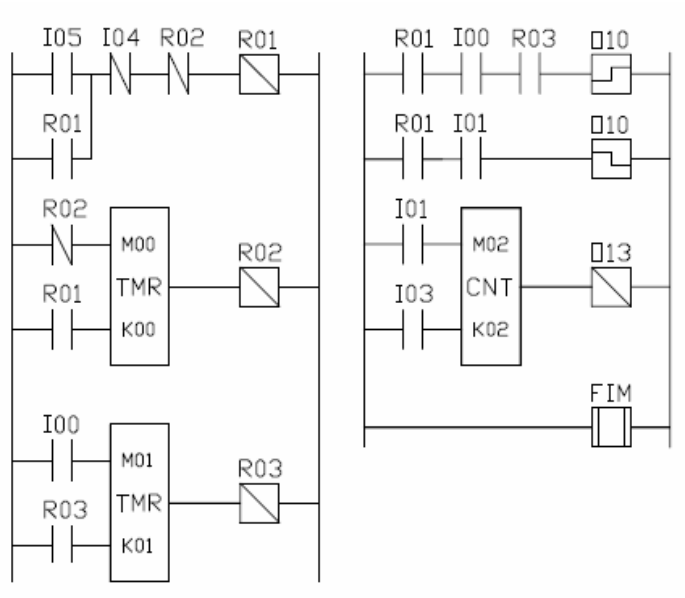

Figure 8: Ladder diagram used to control the applied pressure

Referring to the ladder diagram in Figure 8, a brief explanation is presented here. The switch I05 starts the process activating the relay R01. To control the pneumatic cylinder movement, an inductive sensor (I01) is used to detect the end-of-course of the piston, and other sensor (I00) to detect its initial position. When the sensor I01 is activated, the cylinder returns to its initial position. A timer (TMR0) determinates the period between each piston triggering and consequently the pumping frequency. Another timer (TMR1) determinates the total time of the test, adopted in this case as one minute for all tests. A counter (CNT) was used to confirm the number of piston strokes of the test.

5. ANALYSIS OF THE EXPERIMENTAL RESULTS

Several sets of measurements were conducted to evaluate the prototype performance, described at this section. The applied pressure range varies from 0.1115 to 0.1217 of the ambient pressure, for eleven different positions of the second syringe, and the pumping frequency varies form 2 to 8 Hz, in steps of 1 Hz. The pumped fluid is tap water. Two other reservoir were used, one to hold the input water at 60 mm higher than the pump, and the output reservoir to collect the pumped water. They were connected through flexible tubes, filled with water. The output of the water is above the second reservoir, and 50 mm higher than the pump. This difference was experimentally adjusted just to avoid dropping water due to gravitational pressure difference. This means that any fluid flow is due exclusively to the pumping, and all work made by the pump is converted into flow movement. The results are presented in two graphs, in Figure 9 and Figure 10.

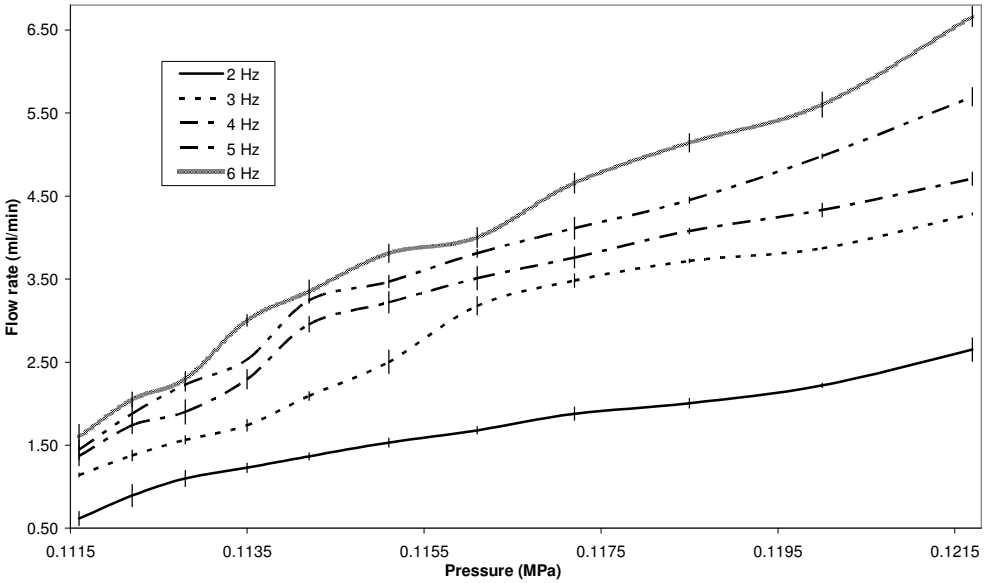

Figure 9: Measured flow rate depending on pressure and pumping frequency

Five curves are represented in Figure 9, relating the applied pressure difference, the pumping frequency and the resulting measured flow rate. Each point in the curve corresponds to ten different measurements for the same applied pressure, and the respective standard deviation is represented also. The flow rate varies from 0.6 ml/min to 6.7 ml/min, respectively the minimum applied pressure difference and 2 Hz pumping frequency, and the maximum pressure difference and 6 Hz. An almost linear behavior may be inferred from the curves, for the range of variables adopted in the test. The effect of increasing the pumping frequency implies a higher flow rate for the same pressure difference.

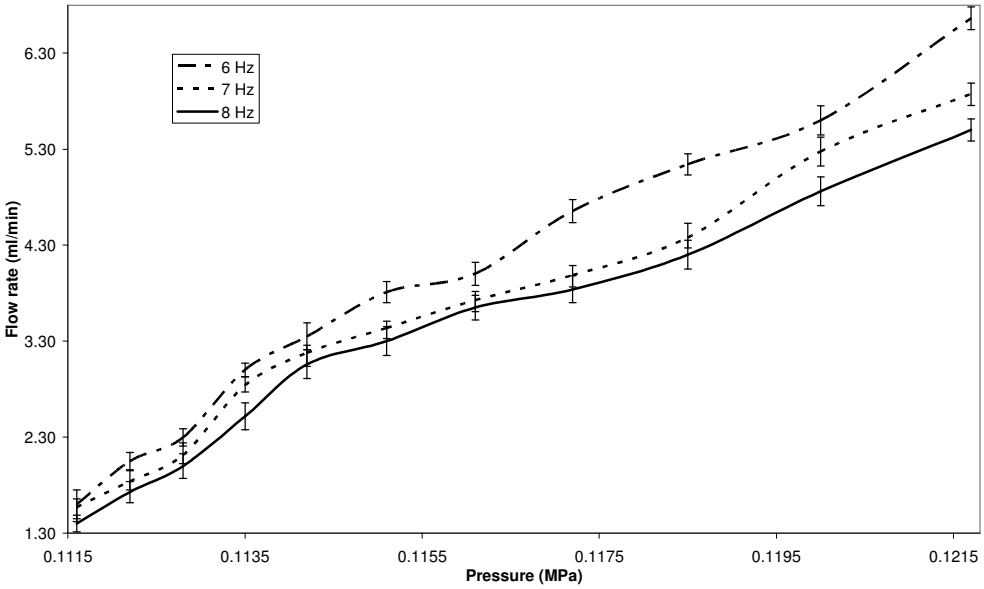

Figure 10: Measured flow rate for higher frequencies

In Figure 10, the procedure to obtain the curves is the same describe above, but the values of pumping frequencies are 6, 7 and 8 Hz, in order to clearly expose an interesting inversion in the variation of flow rate. The behavior of the flow rate is similar to the previous curves, but for the two higher frequencies the flow rate decreases with the increasing of the pumping frequency. To better analyze this fact, new curves were produced with the same data, presented in Figure 11.

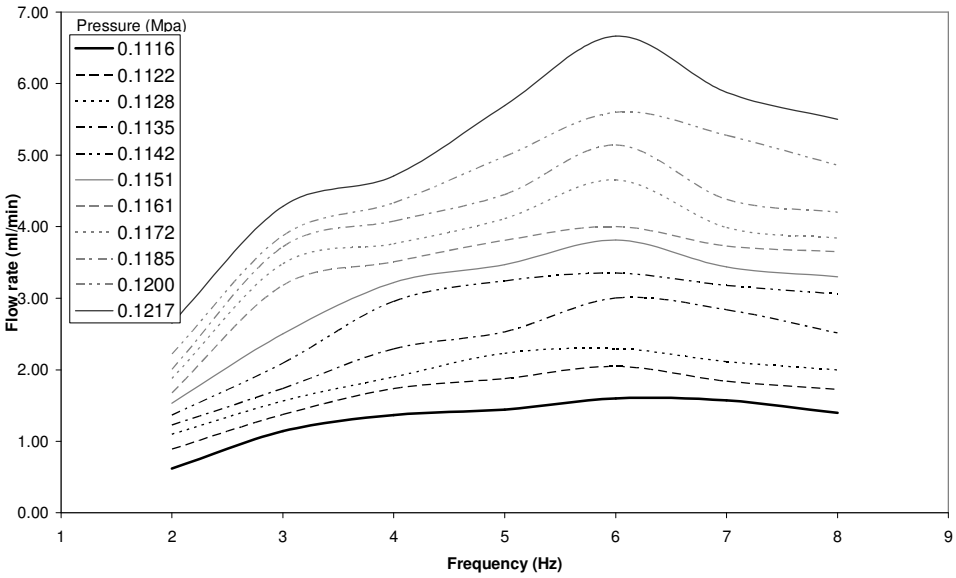

Figure 11: Flow rate data including all frequencies for eleven pressure differences

In Figure 11, the horizontal axis is now the pumping frequency and each curve represents an applied pressure difference. It may be seen that all curves passes through a peak around 6 Hz, decreasing when the frequency is augmented. This pumping frequency compromise was found also in other published results. Yoo *et al* (2006) shows the maximum outflow at 5 Hz frequency and Yang and Jeong (2000) obtained maximum outflow at 3 Hz using a flat diaphragm similar to the one used in this study. Working with a two valves micropump, Zengerle *et al* (1995), noticed the same phenomenon, observing the inversion of the flow in high frequencies. This indicates a limit for the pumping flow rate. Comparing to the referenced cases, the result indicates a larger actuation possibility for the micropump here presented. A possible explanation for the flow rate peak is the natural frequency of the second order membrane. Further studies are necessary to evaluate the mechanical properties of the membrane material and mounting, and confirm the frequency value.

To verify the influence of both parameters together, a 3D graphic with all data is presented in Figure 12.

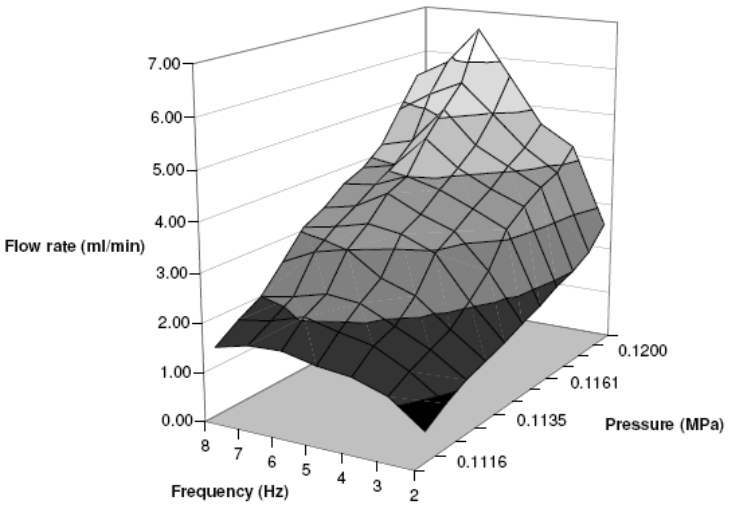

Figure 12: 3D representation of all experimental data

It is possible to notice in Figure 12 that the maximum flow rate can be obtained using a 6 Hz pumping frequency and a 0.1217 pressure difference. New experimental data would be interesting to investigate the behavior for higher pressure differences, but this maximum value resulted from the limitations of the adopted testing setup.

A PARETO's graphic to study the relative influence of each parameter over the flow rate is presented in Figure 13.

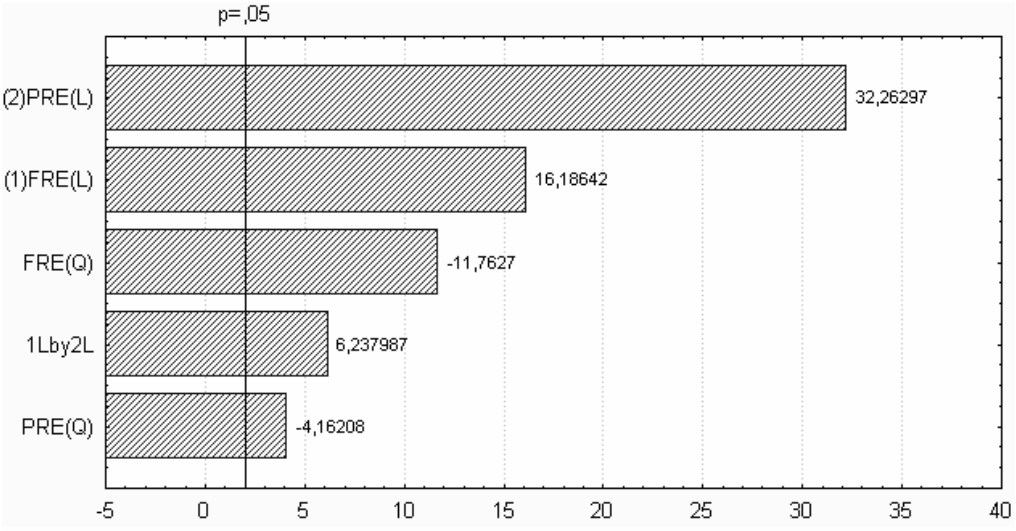

Figure 13: PARETO's graphic analysis

Referring to Figure 13, the first parameter, in descendent order, is the pressure difference, the second is the pumping frequency, the third is the square of the frequency, the forth is the product of pressure and frequency, and the last one is the square of the frequency. It is possible to see that the linear pressure difference is the most influential parameter. It has an influence two times bigger then the pumping frequency (32.263 against 16.187). This means that to increase the flow rate, it is more interesting to increase the pressure difference than the frequency.

6. CONCLUSION

A diaphragm valveless micropump prototype using polyuretano-acrilate as structural material and latex for the membrane was constructed and tested. The adopted fabrication method was chosen considering the possibility of low cost and consequently a future bigger market for an industrial equivalent product. Experimental data shows that the micropump prototype may be considered efficient when compared with similar prototypes presented in literature. The prototype was able to produce flow rate from 0,5 to 6,5 mL with good repeatability. The absence of valves does not reduce the global performance, but it simplifies significantly the manufacturing method. The fabrication technique used guarantees indeed lower cost. The membrane can reach a larger flow rate range then other models that could be found in literature. It is possible to notice that the applied pressure difference is the most important parameter in its performance. The work will continue through developing and validating a bond graph model, in order to better explain the experimental results. Finally, new prototypes using PA also as the membrane material will be designed and tested.

7. AKCNOWLEDGEMENTS

The authors thank the Brazilian agency FAPESP for the financial support for this research work.

8. REFERENCES

Bacher, W.,Menz, W. and Mohr, J., 1995, "The LIGA Technique and Its Potential for Microsystems – A Survey", IEEE Trans. On Industrial Electronics, Vol. 42, pp. 431-441.

Burns, M. A., Johnson, B. N., Brahmasandra, S. N., Handique, K., Webster, J. R., Krishnan, M., Sammarco, T. S., Man, P. M., Jones, D., Heldsinger, D., Mastrangelo, C. H., Burke, D. T., 1998, "Sealed-Cavity Resonant Microbeam Pressure Sensor", Sci., Vol. 282, p. 253.

Bustillo, J. M., Howe, R. T., Muller, R. S., 1998, "Surface Micromachining for Microelectromechanical Systems", Proc. IEEE, Vol. 08, pp. 1552-1574.

Chow, A. W.,2002, "Lab-on-a-chip: Opportunities for Chemical Engineering", AIChE J., Vol. 48, pp. 1590-1595.

Costa, J. N., 2006, "Projeto e Teste de uma Microbomba sem Válvulas",Tese de Mestrado, Univ. Est. Campinas.

Daniel, D., Gutz, I. G. R., 2006, "Eletronic Micropipettor: A Versatile Fluid Propulsion And Injection Device For Micro-Flow Analysis", Anal. Chim. Acta, Vol. 571, pp. 218-227.

Ehrfeld, W., 2003, “Electochemistry and Microsystems”, Electroch. Acta, Vol. 48, pp. 2857-2868.
Fang, J. Wang, K. W., Bohringer, K. F., 2006, “Self-Assembly Of PZT Actuators For Micropumps With High Process Repeatability”, J. Microelectromec. Sys., Vol. 15, pp. 871-878.
Fernandes, J. C. B., Ferreira, L. O.S, 2006, “Manufacturing Of Miniature Fluidic Modules For Lab-On-A-Chip Using UA Photoresin From Flexographic Platemaking Process”, J. of Braz. Chem. Soc., Vol. 17, pp. 643-647.
Feynman, R.P., 1960, “There’s Plenty of Room at the Bottom: An Invitation to Enter a NewWorld of Physics,” 1960 issue of Caltech’s Engineering and Science.
Herr, A., Kenny, T., Santiago, J., Mungal, M. Garguilo, M., 1999, “Variation Of A Capillary Wall Potential In Eletrokinetic Flow”, Transducers, Vol. 1, Sendai, Japan, pp.710-713.
Jiang, X., Zhou, Z., Huang, X., Li, Y., Yang, Y., Liu, C., 1998, “Micronozzle/ Diffuser Flow And Its Application In Micro Valve Less Pump”, Sensors and Actuators A, Vol. Vol. 70, pp. 81-87.
Khoo, M. and Liu, C., 2000, “A Novel Micromachined Magnetic Membrane Microfluid Pump”, An. Int. Conf. IEEE Eng. in Med. and Bio., Vol. 3, pp. 2394-2397.
Ko, J.S., Kim, G.H., Cho, Y. H., Lee, K., Kwak, B. M., Park, K., 1995, “A Self-diagnostic Airbag Accelerometer with Skew-symmetric Proof-mass”, IEEE International Workshop on MEMS, Miami, USA, p.163.
Madou, M.,, 1997, “Fundamentals of Microfabrication” Ed. CRC, New York, USA,589p.
Nathanson, H. C., Newell, W.E., Wickstrom, R.A., Davis, J.R., 1967 “The Resonant Gate Transistor”, IEEE Trans. Elect. Dev. Vol. 14, pp. 117–133.
Nguyen, N. T., Meng, A. H., Black, J., White, R.M., 2000, “Integrated Flow Sensor for In Situ Measurements and Control Of Acoustic Streaming In Flexural Plate Wave Micropumps”, Sens. Act., A, Vol. 79, pp. 115-121.
O’Connor, L., 1992, “MEMs: Microeletricomechanical Systems”, Mech. Eng. – Vol. 114, pp. 40-48.
Olsson, A., 1998, “Valveless Diffuser Micropumps”, Tese de Doutorado, Roy. Inst. of Tech.
Olsson, A., Stemme, G., Stemme, E. 2000, “Numerical and Experimental Studies of Flat-Walled Diffuser Elements For Valves-Less Micropumps”, Sens. Act., A, Vol. 84, pp.165-175.
Petersen, K. E., 1982, “Silicon as a mechanical material”, Proc. IEEE – Vol. 70, pp. 420-457.
Poel Filho, C. J., 2006, “Modelagem Numérica Multi-domínios para Aplicação em Microssistemas Eletromecânicos”, Tese de Doutorado, Univ. Est. Campinas.
Rogers, J. A., Nuzzo, R.G., 2005, “Recent Progress in Soft Lithography”, Mat. Tod. , Vol. 8, pp. 50-56.
Roylance, L, Angell, J., 1978 “A miniature integrated circuit accelerometer” Digest of 1978 IEEE International Solid-State Circuits Conference, pp.220–221.
Schwarz, M. A., Hauser, P. C., 2001, “Recent Developments in Detection Methods for Microfabricated Analytical Devices ”, Lab on a chip, Vol. 1, pp.1-6.
Smits, J. G.,1990, “Piezoelectric Micropump with three Valves Working Peristaltically”, Sensors and Actuators, A, Vol. 21, pp. 203-206.
Smith, C. S., 1954, “Piezoresistance Effect in Germanium and Silicon”, Phys. Rev. - Vol. 94, pp. 42-49.
Stemme, E., Stemme, G. 1993, “A Valvless Diffuser/ Nozzle-based Fluid Pump”, Sensors and Actuators, A, Vol. 21, pp. 203-206.
Teymoory, M. M., Abbaspour-Sani, E. 2005, “Design and Simulation of a Novel Electrostatic Peristaltic Micromachined Pump for Drug Delivery Applications”, Sensors and Actuators, A, Vol. 117, pp. 222-229.
Yamahata, C., Lacharme, F. and Gijs, M. A., 2005, “Glass Valveless Micropumps Using Electromagnetic Actuation.”, J. of Microelectronic Eng., Vol. 78, pp. 132-137.
Yazdi, N., Naijfi, K., 2000, “An All-silicon Single-wafer Micro-g Accelerometer with a Combined Surface and Bulk Micromachining Process.”, Journal of Microelectromechanical Systems, Vol. 9, pp. 544-550.
Yoo, J. C., Moon, M. C., Choy, Y. J, Kang, C. J., Kim, Y. S., 2006, “A High Performance Microfluidic System Integrated with the Micropump and Microvalve on the same Substrate”, Microelectronic Engineering, Vol. 83, pp. 1684-1687.
Zengerle, R., Ulrich, J., Kluge, S., Richter, M., Richter, A., 1995 “A Bi-directional Silicon Micropump”, Sens. Act.A, Vol. 50, pp. 81-86.
Zhang, T., 2005, “Valveless Piezoelectric Micropump for fuel Delivery in Direct Methanol Fuel Cell (DMFC) Devices”, Tese de Doutorado, University of Pittsburgh.

9. RESPONSIBILITY NOTICE

The authors are the only responsible for the printed material included in this paper.